J Electr Eng Technol.2018; 13(2): 822-828
http://doi.org/10.5370/JEET.2018.13.2.822

ISSN(Print) 1975-0102
ISSN(Online) 2093-7423

Robust Control of Current Controlled PWM Rectifiers Using Type-2 Fuzzy Neural Networks for Unity Power Factor Operation

Hakan Acikgoz†, Resul Coteli*, Mehmet Ustundag and Besir Dandil*****

Abstract – AC-DC conversion is a necessary for the systems that require DC source. This conversion has been done via rectifiers based on controlled or uncontrolled semiconductor switches. Advances in the power electronics and microprocessor technologies allowed the use of Pulse Width Modulation (PWM) rectifiers. In this paper, dq-axis current and DC link voltage of three-phase PWM rectifier are controlled by using type-2 fuzzy neural network (T2FNN) controller. For this aim, a simulation model is built by MATLAB/Simulink software. The model is tested under three different operating conditions. The parameters of T2FNN is updated online by using back-propagation algorithm. The results obtained from both T2FNN and Proportional + Integral + Derivate (PID) controller are given for three operating conditions. The results show that three-phase PWM rectifier using T2FNN provides a superior performance under all operating conditions when compared with PID controller.

Keywords: PWM rectifier, Type-2 fuzzy neural network, PID controller, Robust control, Adaptive control

1. Introduction

With development of technology in recent years, the energy demand has been increased and the great majority of this need is electricity. The sources for generation of electricity are limited. The increase in the cost of electricity production has been reflected on the user side and the amount paid to electricity has increased. For this reason, today's electrical devices have been designed to provide high efficiency and power factor [1-5]. Nowadays, it is well- known that electric energy is supplied to users by using power electronics devices such as rectifier and inverter circuits. Such power electronics circuits have to design to operate at unity power factor for high efficiency. Recently, studies on Pulse Width Modulation (PWM) rectifiers have been intensively increased because of their ability such as unity input power factor and approximately sinusoidal AC grid current. PWM rectifiers provide high power factor, low harmonic content of AC side current, bi-directional transmission of the energy, etc [5-7].

Proportional + Integral (PI) and Proportional + Integral + Derivate (PID) controllers are commonly employed to control DC-link voltage and dq-axis current of PWM rectifiers. However, the performances of these controllers are poor because the design of PID controllers depends on the mathematical model of the system to be controlled. A number of control methods and controllers have been proposed for controlling DC-link voltage and dq-axis current of these rectifiers [5]. In Ref. [8], PI-based linear controller was proposed in order to control DC-link voltage and input currents of PWM rectifier with LCL filter. In Ref. [9], fuzzy logic controller was designed as current regulator of PWM rectifier. In Ref. [10], the authors proposed neuro-fuzzy controller for DC-link voltage and dq-axis current of PWM rectifiers. In Ref. [11], dead-beat power control scheme was used in order to demonstrate performance of three-phase AC/DC converters. Experimental studies have been carried out to confirm the validity of the proposed control schema. In Ref. [12], authors presented the predictive current control of three-phase PWM rectifier. Two predictive current control algorithms were proposed to control of input current vector components in the stationary abc and rotating dq reference frame.

Recently, type-2 fuzzy logic systems (T2FLSs) which have ability to cope with the uncertainties in type 1 fuzzy logic systems (T1FLSs) have been used in many applications [13-22]. Artificial neural networks (ANNs) are computer systems used to obtain the ability to discover new information through learning from the characteristics of the human brain without any help. The control systems, which have all the properties of T2FLSs and ANNs, are known as type-2 fuzzy neural networks (T2FNNs). T2FNNs are becoming more powerful for controlling of nonlinear systems [19-23].

In this paper, DC-link voltage and dq-axis current of PWM rectifier are controlled by using T2FNN controller. A simulation model including AC grid, three-phase PWM rectifier, loads and controller unit is built by using Matlab-Simulink software. Reference d-axis current is obtained

† Corresponding Author: Dept. of Electrical Science, Kilis 7 Aralik University, Turkey. (hakanacikgoz@kilis.edu.tr)
* Dept. of Energy Systems Engineering, Firat University, Turkey. (rcoteli@firat.edu.tr)
** Dept. of Electrical and Electronics Engineering, Bingol University, Turkey. (mustundag@bingol.edu.tr)
*** Dept. of Mechatronics Engineering, Firat University, Turkey. (bdandil@firat.edu.tr)
Received: April 19, 2017; Accepted: November 25, 2017

from output of the DC-link voltage controller whereas reference q-axis current is set to zero. To show performance of three-phase PWM rectifier using T2FNN in the voltage and current control loops, different operating conditions are considered. In order to show the high performance and robustness of the T2FNN controller, three different operating conditions as constant reference input, set point changing and input disturbance were determined and the results obtained from these conditions were presented. The compared results were given for T2FNN controller and PID controller.

2. Mathematical Model of PWM Rectifier

Main configuration of three-phase PWM rectifier has been shown in Fig. 1. PWM rectifier consists of six IGBTs and parallel connected six diodes. A capacitor (C) is connected at the DC link as a filter.

Three-phase line voltages (u_{abc}) and the fundamental line currents (I_{abc}) are [1-3]:

$$\begin{bmatrix} u_a \\ u_b \\ u_c \end{bmatrix} = E_m \begin{bmatrix} \cos \omega t \\ \cos(\omega t + 2\pi/3) \\ \cos(\omega t - 2\pi/3) \end{bmatrix} \quad (1)$$

$$\begin{bmatrix} i_a \\ i_b \\ i_c \end{bmatrix} = I_m \begin{bmatrix} \cos(\omega t + \varphi) \\ \cos(\omega t + 2\pi/3 + \varphi) \\ \cos(\omega t - 2\pi/3 + \varphi) \end{bmatrix} \quad (2)$$

Where, ω is angular frequency. Line-to-line voltages of three-phase PWM rectifier can be defined as [1]:

$$\begin{aligned} u_{Sab} &= (S_a - S_b)u_{dc} \\ u_{Sbc} &= (S_b - S_c)u_{dc} \\ u_{Sca} &= (S_c - S_a)u_{dc} \end{aligned} \quad (3)$$

$$\begin{aligned} f_a &= [2S_a - (S_b + S_c)]/3 \\ f_b &= [2S_b - (S_a + S_c)]/3 \\ f_c &= [2S_c - (S_a + S_b)]/3 \end{aligned} \quad (4)$$

Where, S_a, S_b and S_c are switching state of PWM rectifier,

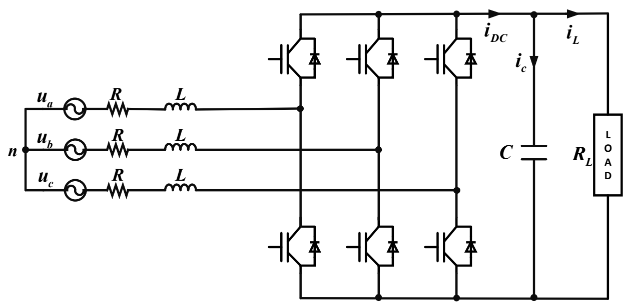

Fig. 1. Configuration of three-phase PWM rectifier

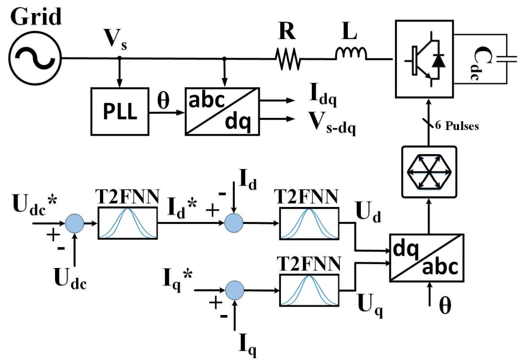

Fig. 2. Control scheme of three-phase PWM rectifier

f_{abc} are assumed to be 0, ±1/3 and ±2/3. The voltage equations for balanced three-phase system in *abc* frame can be written as:

$$\begin{bmatrix} u_a \\ u_b \\ u_c \end{bmatrix} = R \begin{bmatrix} i_a \\ i_b \\ i_c \end{bmatrix} + L \frac{d}{dt} \begin{bmatrix} i_a \\ i_b \\ i_c \end{bmatrix} + \begin{bmatrix} u_{sa} \\ u_{sb} \\ u_{sc} \end{bmatrix} \quad (5)$$

Where, C is DC link capacitor and U_{dc} is DC-link voltage. The equations in the synchronous dq-coordinates are obtained as:

$$C \frac{du_{dc}}{dt} = S_a i_a + S_b i_b + S_c i_c - i_L \quad (6)$$

U_{dc} is DC-link voltage. The equations in the synchronous dq-coordinates are obtained as:

$$\begin{bmatrix} u_d \\ u_q \end{bmatrix} = R \begin{bmatrix} i_d \\ i_q \end{bmatrix} + L \frac{d}{dt} \begin{bmatrix} i_d \\ i_q \end{bmatrix} + \omega L \begin{bmatrix} i_d \\ i_q \end{bmatrix} + \begin{bmatrix} u_{sd} \\ u_{sq} \end{bmatrix} \quad (7)$$

$$C \frac{du_{dc}}{dt} = \frac{3}{2}(S_d i_d + S_q i_q) - i_L \quad (8)$$

In Eq. 8, i_L is load current.

Fig. 2 shows the proposed control structure for DC-link voltage and dq-axis current of three-phase PWM rectifier. The output of T2FNN used in DC-link voltage is d-axis current whereas the outputs of T2FNNs used in dq-axis current are V_q and V_d voltages. The reference value of the q-axis current is set to zero for the unity power factor operation..

3. Type-2 Fuzzy Neural Network System

Fuzzy neural networks (FNNs), which have all the properties of FLSs and ANNs in a single structure, are widely used [19-23]. Type-2 FLSs have been proposed in many areas, such as forecasting of time series, controlling of mobile robots, and the truck backing-up control problem

[13-17]. In design of type-1 FLSs, the designer faces some significant problems, which are uncertainties that arise when defining the rules and determining the parameters of membership functions (MFs). In the rules, the uncertainties may arise in the premise and consequent linguistic descriptions of the rules depending on experts. In MFs, problems are encountered in determining the exact values of the MFs and their parameters. Because of these problems, type-1 FLSs may encounter uncertainties such as measurement noises, changes in operating conditions of the controller, and disturbance effects on the system. Such uncertainties can be assumed as MF uncertainties in type-2 FLSs. With such planning, the MFs used in type-2 FLSs include infinite type-1 as MF within the specified range. This advantage of type-2 FLSs can reduce adverse effects of uncertainties such as modelling errors, parameter and load changes, and noise on system. T2FNN structure consisting of a multi-input single- output is given in Fig. 3. The premise parts of T2FNN are formed from fuzzy sets with type-2, which are characterized by uncertain means and fixed standard deviations (STDs). The consequent part of fuzzy rule is of a Takagi-Sugeno-Kang (TSK) type that accomplishes a linear combination of input variables obtained from interval set. T2FNN rules in this paper can be given in Eq. 9.

$$\begin{aligned} &If\ x_1\ is\ \tilde{B}_1^i,\dots,x_m\ is\ \tilde{B}_m^i \\ &Then\ y_j is\ \tilde{a}_0^i+\sum\nolimits_{j=1}^{m}\tilde{a}_j^i x_j, \mathrm{i}=1,\cdots,m,\ j=1,\cdots,m \end{aligned} \tag{9}$$

Where, $\tilde{a}_j^i=[c_j^i-s_j^i, c_j^i+s_j^i]$. Input variables are symbolized as $x_1,\dots, x_m$. $\tilde{B}_1^i$ is type-2 MF. Gaussian type MF with uncertain mean is preferred in this study. The mathematical equation of Gaussian MF can be expressed as [23]:

$$\mu(x)=\exp\left(-\frac{1}{2}.\frac{(x-z)^2}{\rho^2}\right)\equiv G(x,z,\rho) \tag{10}$$

Where; z is the mean value, ρ is STD and x is the input variable. Layer 1 is known as the input layer of T2FNN. As shown in Fig. 3, the outputs of this layer is transmitted as input to the layer 2 and layer 4. Layer-2 introduces linguistic term and the fuzzification operation is fulfilled with preferred MFs in this layer. Layer 3 is known as the firing layer of T2FNN. Each node in layer 3 describes a fuzzy rule and calculates the firing strength. The firing strength is can be found by the following equation.

$$F_j=\left[\underline{f}_j,\overline{f}_j\right],\ j=1,\dots,m \tag{11}$$

$$\underline{f}_j=\prod_{i=1}^{n}\mu_{ij},\ \overline{f}_j=\prod_{i=1}^{n}\mu_{ij},\ i=1,\dots,n \tag{12}$$

Layer 4 is called as the consequent layer of T2FNN. The output of each node is a type-1 fuzzy set, which can be called TSK-type weights. TSK-type weights can be calculated as:

$$\left[w_{jl},\mathrm{w}_{jr}\right]=\left[c_{0j}-s_{0j},\mathrm{c}_{0j}+s_{0j}\right]+\sum_{i=1}^{n}\left[c_{ij}-s_{ij},c_{ij}+s_{ij}\right]x_i \tag{13}$$

Where, consequent parameter is as c_{ij} and s_{ij}. And the output of layer 4 can be represented as:

$$w_{jl}=\sum_{i=0}^{n}c_{ij}x_i-\sum_{i=0}^{n}s_{ij}\left|x_i\right| \tag{14}$$

$$\underline{f}_j=\prod_{i=1}^{n}\underline{\mu}_{ij},\ \overline{f}_j=\prod_{i=1}^{n}\overline{\mu}_{ij},\ i=1,\dots,n \tag{15}$$

Layer 5 is known output processing layer or type reduction layer of T2FNN. The output function consists of the output of layer 3 and layer 4. The design factors (q_l, q_r) allow the upper and lower values to be adjusted adaptively. The outputs (y_l, y_r) can be found as:

$$y_l=\frac{\left(1-q_l\right)\sum_{j=1}^{m}\overline{f}_j w_{jl}+q_l\sum_{j=1}^{m}\underline{f}_j w_{jl}}{\sum_{j=1}^{m}\left(\underline{f}_j+\overline{f}_j\right)} \tag{16}$$

$$y_r=\frac{\left(1-q_r\right)\sum_{j=1}^{m}\underline{f}_j w_{jr}+q_r\sum_{j=1}^{m}\overline{f}_j w_{jr}}{\sum_{j=1}^{m}\left(\overline{f}_j+\underline{f}_j\right)} \tag{17}$$

Layer-6 containing two summation blocks is called output layer of T2FNN. The node in this layer calculate the output variable with the help of defuzzification operation. The following equation gives the defuzzified output:

$$y=y_l+y_r \tag{18}$$

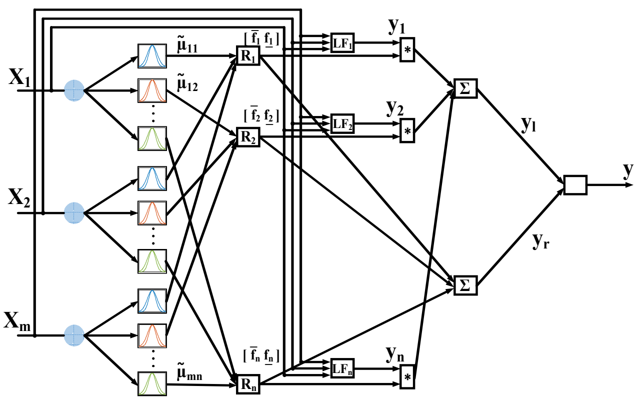

Fig. 3. The structure of T2FNN

4. Simulation Studies

In this section, performance of three-phase PWM rectifier is evaluated in Matlab/Simulink environment. Firstly, the gain parameters of PID controller are empirically found for the voltage and current loops of PWM rectifier via Cohen-Coon method in order to minimize steady state errors and load disturbances. For this aim, system is considered a first-order dead time transfer function ($Ke^{-\tau_d s} / \tau s + 1$). Then, the proposed T2FNN controller is designed and trained until the desired performance is obtained. The parameters of three-phase PWM rectifier and proportional gain (K_p), integral gain (K_i) and derivative gain (K_d) of PID controller are summarized in Table 1. Three scenarios have been carried out to illustrate the dynamic performance of three-phase PWW rectifier. These scenarios have been selected as constant reference input for DC link voltage, step command for DC link voltage and voltage sag condition in AC side. Figs. 4-6 show the simulation results related to these scenarios. These figures consist of DC-link voltage, grid current and voltage, reactive power and active power components. Transient and steady state response of three-phase PWM rectifier are investigated for all scenarios. All voltage and current waveforms are assumed to be 1 and 0.4 p.u, respectively.

The first scenario is realized in order to demonstrate the dynamic performance of the proposed T2FNN controller in both transient and steady state operations. In this scenario, DC link voltage is set to 400V. As shown in Figs. 4(a) and (e), DC link voltage response of three-phase PWM rectifier using T2FNN follows perfectly the reference DC-link voltage without overshoot. In case of PID controller, DC link voltage tracks the reference DC link voltage with overshoot. The settling times of PID and T2FNN controllers are approximately 0.1 and 0.03 s, respectively. Figs. 4(b) and (f) indicate the grid voltage and current waveforms. As seen from the figure, current and voltage are in the same phase. Figs. 4(c)-(g) and (d)-(h) show the waveforms of reactive power component (I_q) and active power component (I_d). In order to achieve unity power factor, reactive power component (I_q) is to zero.

The second scenario is carried out in order to demonstrate the performances of both controllers under the DC link reference changes. As shown in Figs. 5(a) and (e), firstly, the reference DC link voltage is set to 400 V. Then, the reference DC link voltage is increased to 500 V in 0.35 s. Finally, DC link voltage is reduced to 400 V in 0.7 s. The settling times of DC-link voltage obtained from proposed controller are 0.023 and 0.012 s, respectively while the settling times of PID controller are 0.077 and 0.07 s. Figs. 5(b) and (f) indicate the AC grid voltage and current waveforms. When the reference DC-link voltage reaches its set value, phase of voltage is the same as the phase of the current. However, the voltage and current waveforms obtained from PID controller are not in phase for a very short time. Figs. 5(c)-(g) and Figs. 5(d)-(h) show the waveforms of reactive power component (I_q) and active

Table 1. PWM rectifier simulation parameters

Parameter	Value	Controller	
Line voltage	130 V	K_p	0.42
DC-link Voltage	400 V	K_i	20
Source inductance	5 mH	K_d	0.015
Source resistance	0.1 Ω		
DC-link capacitor	3.3 mF		
Grid frequency	50 Hz		

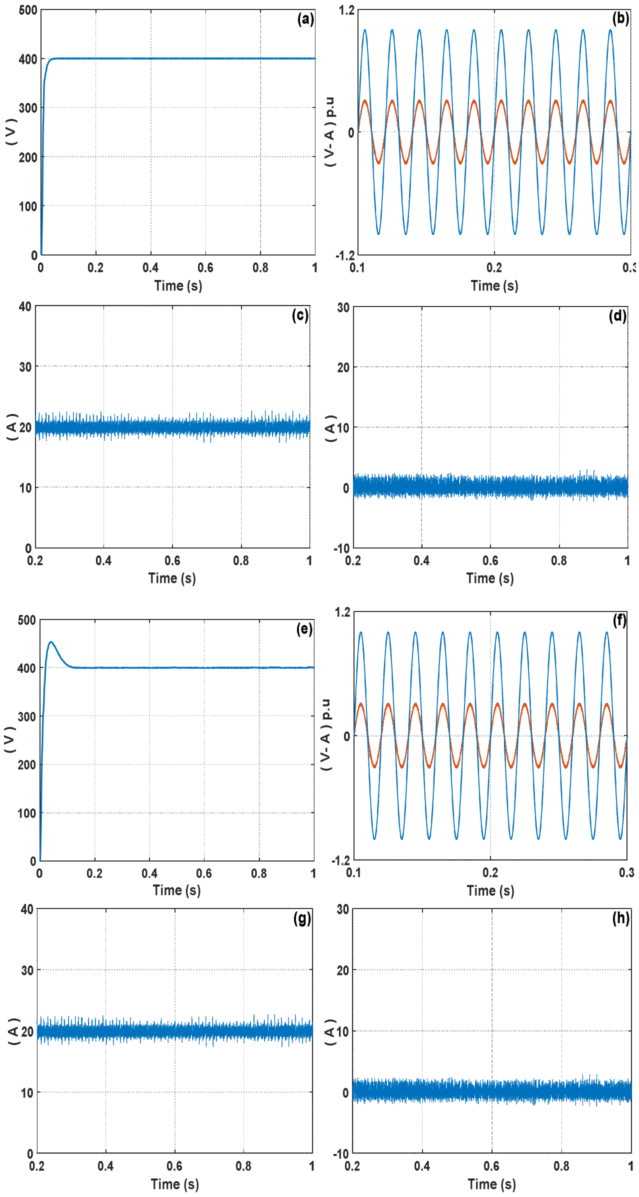

Fig. 4. Waveforms of three-phase PWM rectifier in first scenario (a) DC-link voltage, (b) Grid current and voltage (c) Active power component I_d (d) Reactive power component I_q (T2FNN), (e) DC-link voltage, (f) Grid current and voltage (g) Active power component I_d (h) Reactive power component I_q (PID Controller)

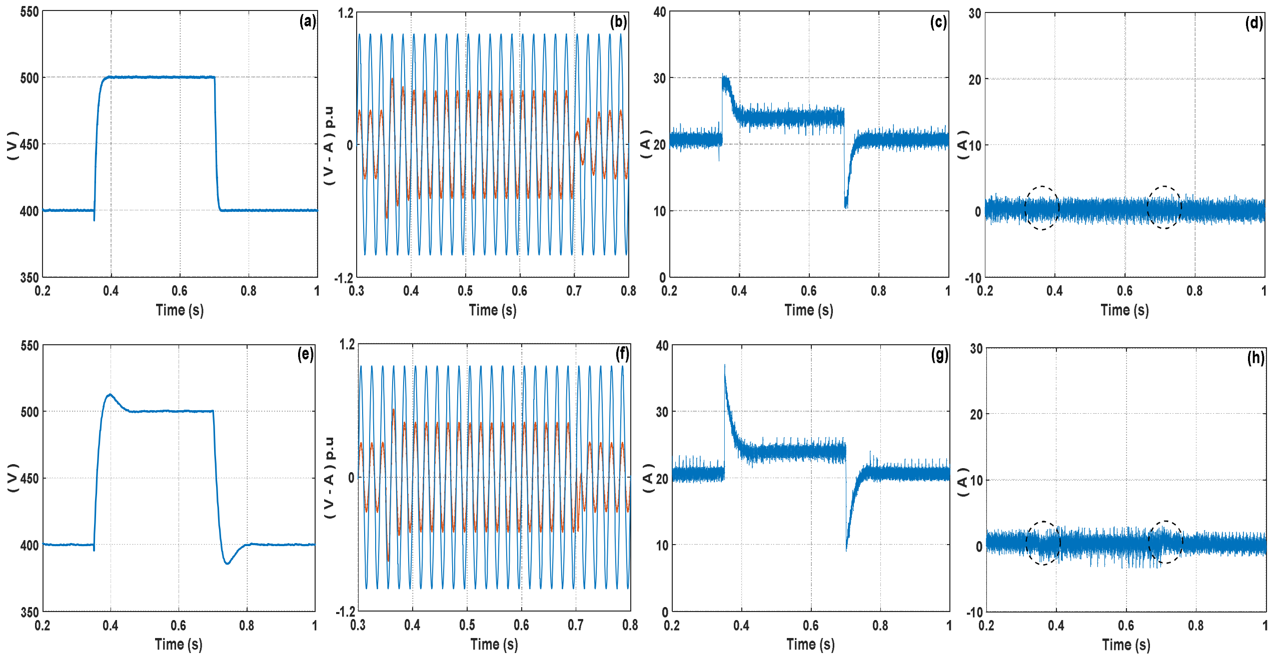

Fig. 5. Waveforms of three-phase PWM rectifier in first scenario (a) DC-link voltage, (b) Grid current and voltage (c) Active power component I_d (d) Reactive power component I_q (T2FNN), (e) DC-link voltage, (f) Grid current and voltage (g) Active power component I_d (h) Reactive power component I_q (PID Controller)

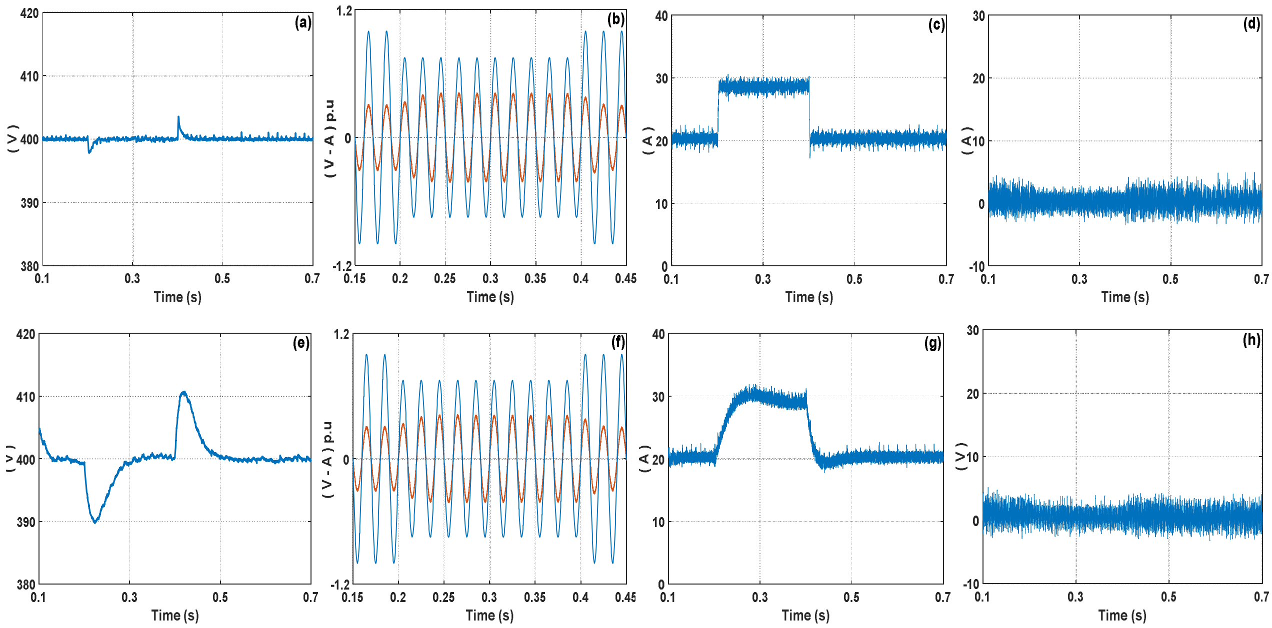

Fig. 6. Waveforms of three-phase PWM rectifier in third scenario (a) DC-link voltage, (b) Grid current and voltage (c) Active power component I_d (d) Reactive power component I_q (T2FNN), (e) DC-link voltage, (f) Grid current and voltage (g) Active power component I_d (h) Reactive power component I_q (PID Controller)

power component (I_d). When these figures are examined, active power component of three-phase PWM rectifier using T2FNN reaches its own value more quickly.

The third scenario is realized to demonstrate the responses of PID controller and T2FNN under voltage sag condition as shown in Fig. 6. In this scenario, AC grid voltage is decreased from 100% to 75% at 0.2 s, and then adjusted to its nominal value at 0.4 s. As shown in Figs. 6(a) and (e), DC link voltage of three-phase PWM rectifier using the proposed T2FNN controller dropped to 398 V and then, it reached its set value at 0.415 s whereas DC link voltage of three-phase PWM rectifier dropped approximately to 390 V in case of PID controller. DC-link voltage reached to set value at 0.5 s. The AC grid voltage and current waveforms are given in Figs. 6(b) and (f). Figs. 6(c)-(g) and Figs. (d)-(h) show the waveforms of reactive power component (I_q) and active power component (I_d). This figure clearly shows that the active power component is perfectly controlled by the proposed T2FNN controller.

5. Conclusion

This paper presents a unity power factor three-phase PWM rectifier using T2FNN in DC link voltage and current control loops. A simulation model including PWM rectifier, T2FNN, load and AC grid is built by using MATLAB/Simulink software. T2FNN current and voltage controlled three-phase PWM rectifier is tested under different operating conditions. Training of T2FNN controller is carried out to obtain the desired performance criteria. The simulation studies have been done in order to evaluate the performance of T2FNN current and voltage controlled PWM rectifier. The results are given as compared with PID controller. The simulation results show that T2FNN controlled PWM rectifier has provided a good and effective performance under different operating conditions and is better dynamic performance when compared with classical PID controller.

References

[1] V. Blasko, V. Kaura, "A new mathematical model and control of a three-phase AC-DC voltage source converter," *IEEE Transactions on Industrial Electronics*, 12, pp. 116-123, 1997.

[2] R. Wu, S.B. Dewan, G.R. Slemon, "Analysis of an AC-to-DC voltage source converter using PWM with phase and amplitude control," *IEEE Trans Ind. Appl.,* 27, pp. 355-364, 1991.

[3] B. Singh, B.N. Singh, A. Chandra, K. Al-Haddad, A. Pandey, D.P. Kothari, "A review of three-phase improved power quality AC-DC converters," *IEEE Transactions on Industrial Electronics,* 51, pp. 641-660, 2004.

[4] M. Sekkeli, H. Acikgoz, O.F. Kececioglu, A. Gani, "Modeling and analysis of three-phase space vector pulse width modulation based rectifiers using fuzzy-PI Controller," *Int Refereed J Eng Sci,* 3, pp. 75-92, 2015.

[5] O.F. Kececioglu, H. Acikgoz, C. Yildiz, A. Gani, M. Sekkeli, "Power Quality Improvement Using Hybrid Passive Filter Configuration for Wind Energy Systems," *Journal of Electrical Engineering & Technology,* 12(1), pp. 206-217, 2017.

[6] Y. Cho, H. Mok, J.S. Lai, "Analysis of the Admittance Component for Digitally Controlled Single-Phase Bridgeless PFC Converter," *Journal of Power Electronics,* 13(4), pp. 600-608, 2013.

[7] A. Emrani, M. Mahdavi, E. Adib, "Soft Switching Bridgeless PFC Buck Converters," *Journal of Power Electronics*, 12(2), pp. 268-275, 2012.

[8] A. Marzouki, M. Hamouda, F. Fnaiech, "A hybrid controller for PWM active rectifiers based LCL filters", *COMPEL: The International Journal for Computation and Mathematics in Electrical and Electronic Engineering,* 34(4), pp. 1229-1251, 2015.

[9] S. Saetieo, D.A. Torrey, "Fuzzy logic control of a space-vector PWM current regulator for three-phase power converters," *IEEE Transactions on Power Electronics*, 13(3), pp. 419-426, 1998.

[10] H. Acikgoz, O.F. Kececioglu, A. Gani, C. Yildiz, M. Sekkeli, "Improved control configuration of PWM rectifiers based on neuro-fuzzy controller," *Springer Plus*, 5(1) pp. 1-18, 2016.

[11] Y. Zhang, W. Xie, Y. Zhang, "Deadbeat direct power control of three-phase pulse-width modulation rectifiers," *IET Power Electronics*, 7(6), pp. 1340-1346, 2014.

[12] A. Bouafiaa, J.P. Gaubert, F. Krim, "Design and implementation of predictive current control of three-phase PWM rectifier using space-vector modulation (SVM), *Energy Conversion and Management*, 51 (12), pp. 2473-2481, 2010.

[13] A. Khosravi, S. Nahavandi, "Load Forecasting Using Interval Type-2 Fuzzy Logic Systems: Optimal Type Reduction," *IEEE Transactions on Industrial Informatics*, 10(2), pp. 1055-1063, 2014.

[14] S.K. Raju, G.N. Pillai, "Design and Implementation of Type-2 Fuzzy Logic Controller for DFIG-Based Wind Energy Systems in Distribution Networks," *IEEE Transactions on Sustainable Energy*, 7(1), pp. 345-353, 2016.

[15] C.S. Chen, "Supervisory adaptive tracking control of robot manipulators using interval type-2 TSK fuzzy logic system," *IET Control Theory & Applications*, 5(15), pp. 1796-1807, 2011.

[16] S. Barkat, A. Tlemçani, H. Nouri, "Noninteracting Adaptive Control of PMSM Using Interval Type-2 Fuzzy Logic Systems," *IEEE Transactions on Fuzzy Systems,* 19(5), pp. 925-936, 2011

[17] F.J. Lin, P.H. Chou, "Adaptive Control of Two-Axis Motion Control System Using Interval Type-2 Fuzzy Neural Network," *IEEE Transactions on Industrial Electronics,* 56(1), pp. 178-193, 2009.

[18] L.A. Zadeh, "Fuzzy sets," *Information and Control,* 8(3), pp. 338-353, 1965.

[19] L.A. Zadeh, "The concept of a linguistic variable and its application to approximate reasoning-I," *Information Sciences,* 8(3), pp. 199-249, 1975.

[20] S. Hassan, M.A. Khanesar, E. Kayacan, J. Jaafar, A. Khosravi, "Optimal design of adaptive type-2 neuro-fuzzy systems: A review," *Applied Soft Computing*, 44, pp. 134-143, 2016.

[21] A. Rahib Hidayat, O. Kaynak, "Type 2 fuzzy neural

structure for identification and control of time-varying plants," *IEEE Transactions on Industrial Electronics*, 57:12, pp. 4147-4159, 2010.
[22] R. Coteli, E. Deniz, B. Dandil, S. Tuncer, F. Ata, "Phase Angle Control of Three Level Inverter Based D-STATCOM Using Neuro-Fuzzy Controller," *Advances in Electrical and Computer Engineering*, 12(1), pp. 77-84, 2012.
[23] J.J. Wang, "Adaptive inverse position control of switched reluctance motor," *Applied Soft Computing*, 60:48-59, 2017.

Hakan Acikgoz received the B.Sc. and M.Sc. degrees from Firat University, Elazıg, Turkey, in 2008 and 2010, respectively. He is currently working towards to the Ph.D degree in Electrical and Electronic Engineering and he is a lecturer at Kilis 7 Aralik University. His research interests are power electronic converters, electronic power transformers, artificial neural networks and fuzzy logic controller.

Resul Coteli received the B.Sc. and M.Sc. degrees in Electrical Education in 2000 and 2006, respectively and the Ph.D. degree in Electrical and Electronics Engineering in 2010, from Firat University, Elazig, Turkey. His research at Department of Energy Systems Engineering interests include applications of power in distribution system, Flexible AC Transmission System (FACTS) devices and Fuzzy Logic control.

Besir Dandil received the B.Sc, M.Sc and PhD degrees in electrical and electronic engineering from Firat University, Elazig, Turkey, in 1992, 1998 and 2004, respectively. Currently, he is a professor at the same university. His research interests include high performance control of induction motors, identification and control of nonlinear systems including artificial neural network and fuzzy control.

Mehmet Ustundag received his bachelor's degree in electronics and computers education from Firat University, Turkey, in 2002, and master's degree from Firat University in 2006. He became a research assistant in the Technical Education Faculty of Firat University in February 2004. He obtained a PhD degree from the Department of Electrical-Electronics Engineering, Engineering Faculty, Firat University. His research interests include signal processing and FPGA.